Research Article

Supeng Deng, Cheuk Ming Mak*, Kuen Wai Ma and Lei Gao

The acoustic effects of temporal and spectral characteristics on traffic sound sensitivity

https://doi.org/10.1515/noise-2025-0020
Received March 30, 2025; accepted September 29, 2025;
published online February 2, 2026

Abstract: Traffic noise is the common component at road intersections in the outdoor environment, and the sounds of traffic light signals are designed to distinguish signal transition between red and green. However, the sounds of traffic light signals are often masked by high levels of vehicle noise produced by high traffic flow. Therefore, this study aims to investigate the acoustic effects of traffic light signals and noise on sound sensitivity in the outdoor environment. A set of psychoacoustic indicators were applied to assess the traffic noise consisting of traffic light signals and vehicle noise at road intersections in Hong Kong. Furthermore, the subjective listening tests evaluated the acoustic sensitivity and perceptions. The results of psychoacoustic time-varying curves revealed distinct characteristics of traffic light signals, with fluctuation strength differing significantly between red and green signals. Moreover, the subjective perceptions of rapid tempo and regularity were significantly correlated with the measured fluctuation strength and rhythmic events per minute (REPM) during the signal transition. These findings will be the insight into the acoustic interactions between various sound sources and their perceptual implications in the outdoor environment.

Keywords: traffic noise; traffic light signals; psychoacoustics; sound sensitivity; temporal characteristics; acoustic environment

1 Introduction

Traffic noise (or traffic sound) is the most common component of environmental noise worldwide [1, 2]. According to European agency assessments, noise pollution has become the second-highest environmental risk after air pollution [3–5]. Hong Kong is a metropolitan area in East Asia with an extremely high population density, and residents face significant health impacts of noise due to its limited urban space and narrow streets [6, 7]. Excessive traffic noise has been reported, and several suggestions have been made to improve the acoustic environment in Hong Kong [8–10]. Related studies involving field measurement and numerical models have been conducted to guide the traffic noise control [11–15]. Among various urban zones, road intersections (crossroads) are critical for traffic noise control due to higher vehicle noise levels produced by high-density vehicles. As another significant sound source at intersections, the traffic light signals (audible traffic signals) are often overlooked in acoustic environment. The traffic light signals are designed to assist visually impaired individuals by automatically adjusting their sound pressure level (SPL) based on the ambient noise level – louder in noisy environments and quieter in calm ones [16].

Previous investigations have evaluated the acoustic effect of traffic light signals. Researchers have reported that higher annoyance ratings at road intersections, compared to the roundabouts without traffic light signals [17]. Numerical simulations of traffic light signals suggested that maximizing the signal-to-noise ratio, using steady and regular frequency tones, is the most effective strategy [18]. The approach has been further validated through a listening test considering the influence of layout on traffic light signals [19]. Subjective listening tests indicated that traffic light signals have minimal impact on indoor residents due to the rapid attenuation of high frequencies [20]. Additionally, measurements showed that the frequency of traffic noise and signal sounds all widely ranged from 400 to 3,000 Hz, with potential differences between the red-light and green-light signals [21, 22]. However, the temporal and spectral characteristics of traffic signal sounds in noisy urban environments remain insufficiently investigated. Moreover, the acoustic difference between traffic signal tones and vehicle noise has not been clearly analyzed in existing research. The complex building layouts and urban canyon effects can also influence

***Corresponding author: Cheuk Ming Mak**, Department of Building Environment and Energy Engineering, The Hong Kong Polytechnic University, Hong Kong, China, E-mail: cheuk-ming.mak@polyu.edu.hk
Supeng Deng, **Kuen Wai Ma and Lei Gao**, Department of Building Environment and Energy Engineering, The Hong Kong Polytechnic University, Hong Kong, China. https://orcid.org/0000-0001-7784-0700 (K.W. Ma)

sound propagation and the perceptibility of traffic signals, especially in complex urban settings like Hong Kong.

In recent years, psychoacoustics has explored the characteristics of human sound perception across various fields [23]. The perceived sound sensitivity of humans can be evaluated by calculating multiple psychoacoustic indicators and metrics [24]. Therefore, psychoacoustic indicators are widely applied in the measurement and survey of outdoor environments and soundscapes [25]. Researchers have found that human-environment interactions are a multidimensional psychological process [26, 27]. The design of the subjective psychometric tool can greatly influence the identification of the primary perceptual impacts of traffic noise on occupants [28, 29]. Furthermore, psychoacoustic indicators, such as Loudness (N), Sharpness (S), Fluctuation strength (FS), Roughness (R), and Tonality (T), comprise a series of objective measured indicators that can more accurately predict human perceptual judgments of noise [23]. Psychoacoustic indicators provide a multidimensional assessment of traffic noise that is not limited to the sound pressure or single intensity indicator (like loudness) [29]. The measurement and statistical analysis of traffic noise were studied by different psychoacoustic indicators, and the results showed that the spectral and temporal indicators are correlated to the complex subjective perception [30, 31].

Traffic light signals differ from general traffic noise and natural sounds due to their regular temporal patterns, like the ringing of a bell. Specifically, a single type of intensity-based indicator (SPL or loudness) is insufficient for evaluating the rapid variations in these sounds [32]. Therefore, psychoacoustic indicators that account for short-term temporal variations should be considered for traffic light signals at the intersections. Previous studies have shown that temporal indicators are not dependent on changes of intensity and spectrum [33–36]. The fluctuation strength (FS) is an available indicator to evaluate the short-term acoustic variations based on the modulation frequency. Other temporal indicators are subjective duration and rhythmic events, which are correlated with FS but are rarely applied in traffic noise [23, 34]. The concept of subjective duration suggests that human perception of short-term sound duration does not solely rely on physical duration [23, 36]. Related research indicates that subjective duration can be influenced by the rhythmic events [37, 38]. Among these indicators, the concept of rhythmic events, derived from music and speech, provides a quantitative measure of subjective duration [39]. Therefore, the psychoacoustic indicator of rhythmic events has the potential to assess the short-term temporal variations in traffic light signals [40].

Previous studies typically relied on sound pressure level (SPL) or a single intensity-based indicator (e.g., loudness) to assess noise at intersections. However, intensity-based indicators are mainly influenced by the vehicle noise, and the acoustic effects of traffic light signals are usually ignored. Meanwhile, existing research has not focused on the subjective perceptions of traffic light signals in noisy environments. In line with the research gaps, this study aims to comprehensively evaluate temporal and spectral characteristics of traffic noise, encompassing both traffic light signals and vehicle noise in the outdoor environment. Such an approach of psychoacoustic indicators can provide deeper insights into the acoustic interactions between these sound sources and their perceptual implications. Specifically, this study seeks: (1) to identify the traffic light signals and vehicle noise at intersections in measured recordings; (2) to establish correlations between psychoacoustic indicators and subjective perceptions; (3) to determine which perceptual components and psychoacoustic indicators are most significant in evaluating the sound sensitivity of traffic light signals.

2 Methods

2.1 Objective measurement

Objective measurements were conducted in Hung Hom, Yau Tsim Mong District, where the percentage and number of residents exposed to noise levels exceeding 70 dB(A) are the highest in Hong Kong [10]. Hung Hom, a predominantly residential area in the southeast of the Kowloon Peninsula, connects three subway stations: Hung Hom, Ho Man Tin, and Whampoa. This area experiences heavy pedestrian and commuter traffic, with numerous heavy vehicles, light vehicles, and public buses on the roads. Therefore, four measurement points and a comparative point were selected to access the traffic sound levels at different road intersections, as shown in Figure 1. All measurement points are linked to the major road network, which has a high capacity of traffic flow. According to local authorities in 2022, the annual average daily traffic values are around 10,000, and the maximum road speed limit is 50 km/h. The surrounding buildings of all measured points are adjacent to high-rise residential structures (over 20 floors), and detailed information of all measured points was provided in Appendix A (see Table 6).

The Brüel & Kjær type 2,270 sound level meter and the Brüel & Kjær type 4,189 microphone were used for the measurement. The calibration test was conducted by the Brüel & Kjær type 4,231 sound calibrator, with a stated accuracy of ±0.2 dB. The calibration was performed before and after each measured recordings, and the maximum permissible deviation for accepting a calibration check was

Figure 1: The measurement locations: measurement point 5 is the comparative point. (The width of single traffic lane is 3.5 m).

set to ±0.5 dB. The result showed that the value of the microphone was 46.9 mV/Pa, which basically matched the value of the open-circuit value. As shown in Figure 1, the sound level meter was located at the roadside or the pedestrian refuge island near the waiting line, and it was also close to the sound source of traffic light signals. The height of the sound level meter was set to 1.5 m (±0.2 m), and the horizontal location was equal to the minimum distance from the nearest traffic light signals to the pedestrian waiting area (described by the traffic light distance in Table 2). Before the formal measurements, the pre-inspection visits to all intersections have been conducted to avoid the non-traffic sources in the measured area (e.g., construction noise or human event sounds).

Sound recordings and the root-mean square sound pressure of the traffic noise were recorded to create the audio WAV files with a 48 kHz sample rate, and noise data ranging from 7 to 10 min was recorded at each measurement point. The red-light and green-light signals cycled repeatedly, and the data recordings were divided into separate segments according to the duration of the red-light or green-light signals. The signal transition from red-light to green-light signals is instantaneous, but there is a flashing period (about 5 s) from green-light to red-light signals. The segments that lasted less than 20 s were eliminated for statistical stability because the 10th percentile of segment duration (red-light signals) was 18.2 s. The flashing green-light signals were also ignored in this study due to the short duration.

Tests were conducted separately during the traffic peak time (6 p.m.–9 p.m. on March, 27, 2024) and the off-peak time (1 a.m.–4 a.m. on April, 21, 2024). The measurements were carried out in conditions without any precipitation. The temperature was between 20 and 25°, the relative humidity was less than 90 %, and the wind speed did not exceed 2 m/s (data were obtained in real time from the Hong Kong Observatory Application). Moreover, the pre-measurement found that the perceived characteristics of the traffic-light signal were only minimally affected without a windshield. Therefore, the windshields' protection was not used on the sound level meter's microphone due to the low wind speed. To minimize the effect of wind interference, the mel spectrograms of all segments were examined to reduce the potential wind noise.

All non-traffic events were tagged in the measurement log, and clear data exclusion criteria were established: any tagged segment of impulsive non-traffic noise, including high-level human event sounds and car horns, was excluded from the final analysis dataset. All available segments of audio WAV files were analyzed by the acoustic toolbox in MATLAB 2024b, and the psychoacoustic indicators can be obtained by the built-in MATLAB program. The detailed parameters of calculations and acquisition settings were provided in Appendix A (see Table 5). The A-frequency weighting and the fast time constant was set to the SPL indicators of L_{Aeq} and L_{max}. All the data from statistical analyses were coded and analyzed by the commercial package SPSS, version 27.0.

2.2 Psychoacoustic indicators

A range of psychoacoustic indicators will cover the traditional indicators (L_{Aeq} and L_{Amax}) and the psychoacoustic indicators (N, S, FS, R, T), and the temporal characteristics for all indicators can be recorded by the time-varying curves [23]. The concept of loudness (N) is used to calculate the sound intensity for human perception. The calculation of the loudness model is based on the ISO 532-1 standard [41], and the equation can be expressed as follows:

$$N = \int_0^{24} N' \mathrm{d}z \tag{1}$$

Specific loudness (N') is expressed as a function of the critical band rate (the unit is sone/Bark). The equation of specific loudness can be expressed as:

$$N' = 0.08 \cdot \left(\frac{E_{\mathrm{TQ}}}{E_0}\right)^{0.23} \left[\left(0.5 + 0.5\frac{E}{E_{\mathrm{TQ}}}\right)^{0.23} - 1\right] \tag{2}$$

In this equation, E_{TQ} is the excitation at the threshold in quiet and E_0 is the excitation of the noise corresponding to the reference intensity $I_0 = 10^{-12}\ \mathrm{W/m^2}$.

The indicator sharpness (S) is strongly correlated with the spectral distribution and the spectral centroid (SC). Spectral centroid describes the distribution of power at different frequencies, and the sharpness model (DIN 45692) is defined by an analogous equation [42]:

$$S = 0.11\frac{\int_0^{24\mathrm{Bark}} N' g(z) z \mathrm{d}z}{\int_0^{24\mathrm{Bark}} N' \mathrm{d}z} \tag{3}$$

where $g(z)$ is the function of the additional factor g on the critical-band rate. The value of $g(z)$ is equal to 1 when the critical-band rates are <16 Bark (approximately 3,150 Hz).

Fluctuation strength (FS) is a temporal indicator related to frequency modulation (FM) and amplitude modulation (AM). Fluctuation strength describes how the sound fluctuates perception over time, reaching its maximum near modulation frequency of 4 Hz and decreasing at higher modulation frequencies. Roughness (R) indicates the spectral perception of stimuli with AM or FM rates, and this value reaches its maximum when the frequency modulation is close to 70 Hz. These indicators based on the Zwicker's model can be given as follows [23]:

$$\mathrm{FS} = \frac{0.008 \int_0^{24\mathrm{Bark}} \Delta L(z)\mathrm{d}z}{f_{\mathrm{mod}}/4 + 4/f_{\mathrm{mod}}} \tag{4}$$

$$R = 0.0003 \cdot f_{\mathrm{mod}} \int_0^{24\mathrm{Bark}} \Delta L_E(z)\mathrm{d}z \tag{5}$$

where, ΔL is the temporal masking depth related to the time-varying amplitude, and ΔL_E is the masking depth modified by the 1 kHz pure tone. The integral range of ΔL and ΔL_E can cover the entire critical-band rate. f_{mod} is the modulation frequency, and the unit is Hz.

The rhythmic event can be calculated by the temporal pattern in the loudness curves, and it has a significant correlation with fluctuation strength (FS). Sound signals with a quick rise in the loudness curves will deviate from the physically temporal perception, and a subjectively rhythmic perception can be produced to adapt the human auditory system [23]. The model of the rhythmic event can be defined by the time-varying loudness within a period of time [43]:

$$N_{\mathrm{max}}/N_M \geq 0.43 \tag{6}$$

$$(N_{\mathrm{max}} - N_{\mathrm{min}})/N_M \geq 0.12 \tag{7}$$

$$\Delta t \geq 120\mathrm{ms} \tag{8}$$

where, N_M denotes the loudness curves of the absolute maximum during a total period. N_{max} and N_{min} are the loudness curves of the relative maximum and minimum during a segmental period. Δt is the minimum time gap between two rhythmic events, and its value needs to be greater than the minimum perceptible time gap (120 ms). The whole sound signal can be divided into several segments according to time-varying loudness curves. A single rhythmic event can be determined when the above three conditions are met in each segment, as shown in Figure 2. Finally, the total number of rhythmic events over a period of time can be calculated.

The indicators of Tonality (T), Tone Level (TL), and Tone-to-noise ratio (TNR) are also considered to describe the tone and pitch of the spectral characteristic, and there are significant correlations among these three indicators [31]. According to the ECMA standard, TNR is the tonal measurement related to the background sound level, and it will determine how clear or noticeable an acoustic event is to the listener [44]. The relationship between the tonal sound and background noise is more comprehensively considered in the TNR indicator, and it is suitable for traffic light signals. A discrete tone will be judged as prominent according to the prominence ratio (prominence tone) method if the TNR value is higher than 9 dB.

Previous studies have shown that a fluctuating sound recording does not correspond to the average value of loudness curves but rather to a value near the maximum

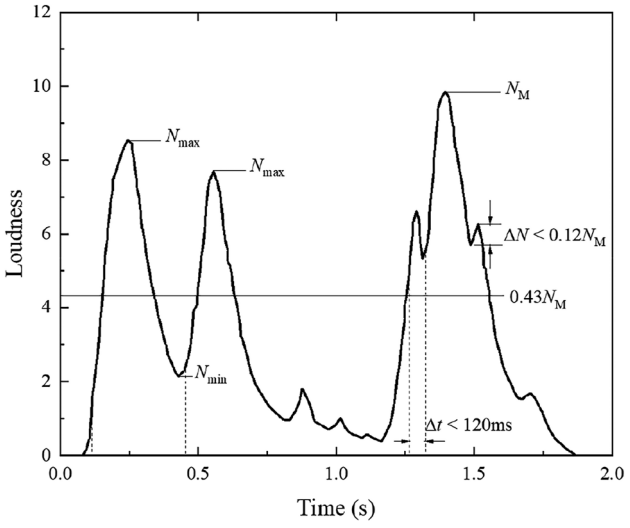

Figure 2: The time-varying loudness curves for showing the example of three calculated rhythmic events.

[23]. Traffic light signals differ from general traffic noise due to their dramatic changes over time. Therefore, the percentile loudness indicator N_5 was used to evaluate traffic noise, where N_5 represents the loudness reached or exceeded within 5 % of the measured time. Furthermore, the aforementioned indicators can be integrated into a comprehensive indicator that describes sound sensitivity and perception. In Zwicker's model, Psychoacoustic annoyance (PA) can quantitatively analyze annoyance ratings in field measurements [23]. Besides intensity indicators like loudness, psychoacoustic annoyance also depends on temporal and spectral characteristics. The equation can be expressed as follows:

$$PA = N_5\left(1 + \sqrt{\omega_S^2 + \omega_{\mathrm{FR}}^2}\right) \tag{9}$$

$$\omega_S = (S - 1.75) \cdot 0.25 \lg(N_5 + 10) \quad S > 1.75 \tag{10}$$

$$\omega_{\mathrm{FR}} = \frac{2.18}{(N_5)^{0.4}}(0.4 \cdot F + 0.6 \cdot R) \tag{11}$$

Where, the value of ω_S is 0 if the S is <1.75. The unit of the PA is sone, which is consistent with the unit of loudness. The psychoacoustic indicators N_5, S, F and R are considered in the PA model, whose units are sone, acum, vacil, asper respectively. To sum up, all psychoacoustic indicators with methods are summarized in Table 1.

2.3 Subjective listening tests

The listening tests were conducted in a quiet room (length 4.2 m × width 3.2 m × height 2.8 m) with a background noise

Table 1: Psychoacoustic indicators with methods.

Psychoacoustic indicators	Measured indicators	Units	Standard or method
Loudness (N)	N_{eq}, N_5, N_{max}	Sone	ISO 532-1 [41].
Sharpness (S)	S_{eq}	Acum	DIN 45692 [42].
Roughness (R)	R_{50}	Asper	Zwicker's method [23].
Fluctuation strength (FS)	FS_{50}	Vacil	Zwicker's method [23].
Rhythmic events	REPM	–	Time-varying loudness definition [43].
Tonality (T)	TNR	dB	ECMA 418-1 [44].
Psychoacoustic annoyance	PA	–	Zwicker's method [23].

level of 39 dB (A). The listener sat in a chair in front of a table, and the indoor air quality is good. Therefore, the participants can concentrate on the recorded segments and give the effective answers. The recorded segments were played back using an acoustic system that included headphones (Sennheiser HD 600), a high-quality sound card (Focusrite Scarlett Solo 3), and a computer. No additional headphone equalization or HRTF correction was applied to preserve the natural response of the Sennheiser HD 600. The linearity of playback chain (Focusrite Scarlett Solo 3 with HD 600) was verified by the given total harmonic distortion plus noise (THD + N < 0.1 % at 1 kHz, 97 dB SPL). All segments were sourced from the segments mentioned in Section 2.1, and the B&K 4101-B in-ear microphone was used to calibrate the sound pressure levels from the headphones. Due to the lower sound pressure levels (−4.4 dB) of off-peak segments in Table 3, the peak and off-peak segments were calibrated using a standard sound source at 60 dB and 65 dB, respectively.

The experimental procedure and the following instructions were given to participants: "You need to evaluate eight recorded segments of urban sound environments. Imagine yourself walking at road intersections and rating your annoyance on a continuous scale ranging from −3 to 3 (7 scales). You can hear each segment three times, and you will not be able to go back to the previous segments if you validate your answer." After hearing a background traffic

Table 2: The semantic questions in the questionnaire: the score scale for all questions is −3 to 3.

Questions	Question number	Adjective pairs
Annoyance of overall traffic noise	1	Not annoyed – annoyed
Sensitivity to overall traffic noise	2	Not sensible – sensible
Sensitivity to vehicle noise	3	Not sensible – sensible
Sensitivity to traffic light signals	4	Not sensible – sensible
Sensitivity to other sounds	5	Not sensible – sensible
Different perceptions of the traffic noise	6	Pleasant – unpleasant[a]
	7	Relaxed – tense[a]
	8	Light – heavy[a]
	9	Quiet – loud[a]
	10	Monotonous – vibrant[b]
	11	Dull – sharp[a]
	12	Deep – metallic[a]
	13	Low – high[a]
	14	Steady – fluctuant[c]
	15	Regular – irregular[c]
	16	Arhythmical – rhythmic[c]
	17	Slow tempo – fast tempo[c]

"[a]"Denotes the adjective pair recommended by EPA model. "[b]"Denotes the adjective pair recommended by ISO 12913-3; "[c]"denotes the adjective pairs from signal-related research.

Table 3: The information of traffic light segments the measurement points.

Measured point	Traffic light distance (m)	Types of measurement	Number of segments (red/green)	Total SPL L_{Aeq} (dB)	Total elapsed duration (s)
1	0.5	Peak	4/4	71.8	345
		Off-peak	4/5	64.1	366
2	0.5	Peak	3/3	75.2	360
		Off-peak	5/5	64.5	527
3	0.5	Peak	3/3	69.2	463
		Off-peak	5/3	63.2	524
4	2	Peak	5/4	72.1	600
		Off-peak	–	–	–
Total	–	Peak	15/14	71.9	1768
		Off-peak	14/13	63.9	1,417
			29/27	68.3	3,185

1. Traffic light distance: the minimum distance from the nearest traffic light signals to the measurement point. 2. Types of measurement: Peak time (6 p.m.–9 p.m. on March, 27, 2024); off-peak time (1 a.m.–4 a.m. on April, 21, 2024). 3. Total elapsed duration: the sum of measured durations for all segments.

sound (without traffic light signals), eight sound segments were played one by one in random order, and each segment lasted 40–60 s. The tests for each participant lasted approximately 15–20 min. Total 15 participants (13 male and two female), with normal hearing and stable emotion, participated the tests. All participants were aged between 20 and 30 years to control the similar auditory acuity. The participants were asked to score their annoyance, sensitivity, and perceptions by different semantic adjective pairs in Table 2. The answer scale in Table 2 refers to the three-dimension model (EPA model) [25]. The EPA model evaluated the human perceptions about the general judgement, the energy content, and the temporal and spectral content of sound, respectively [45]. Moreover, several additional adjective pairs, including the pairs recommended by the standard ISO 12913-3, were also added to consider the signal-related perception [17, 46–50].

3 Objective results

3.1 Temporal characteristics

3.1.1 Time-varying curves of measured indicators

There were 29 and 27 available segments of red-light signals and green-light signals, respectively, as shown in Table 3. The off-peak segments at measurement point 4 were excluded due to the lower volume of the traffic-light signals. Consecutive segments at measurement point 2 were selected to specifically highlight the temporal trend in the objective results. Four time-varying curves of measured indicators at measurement point 2 for two consecutive segments were presented in Figure 3, and the red lines represent the signal transition from the red signal to the green signal. The time-varying curves of SPL and N in Figure 3(a and b) fluctuated significantly during the red-light signals but remained relatively steady during the green light.

The difference in traffic noise between peak and off-peak times was also significant in Figures 3 and 4. During the off-peak times, the time-varying curves of SPL and N remained relatively flat due to the reduced traffic light volume and vehicle noise. The temporal envelope of red-light signals showed sharp fluctuations, particularly in loudness. In Figure 4(a), the different temporal envelopes of red-light and green-light signals disappeared, but this difference persisted in Figure 4(b). It indicated that the patterns of the time-varying N differ significantly between the red-light and green-light signals. Comparatively, the actual perception of people (N result) is more sensitive than the physical energy change (SPL result) for traffic light signals [23].

Figures 3(c) and 4(c) illustrated the time-varying FS curves of typical results. During the green-light signals, FS values peaked at approximately 0.3 vacil with a steady modulation frequency (f_{mod}) of 12.8 Hz. In contrast, during the red-light signals, FS values fluctuated and dropped to around 0.15 vacil. It indicated a clear difference in the temporal patterns during the signal transition, with an inverse relationship between N and FS in Figure 3(b) and (c). The temporal envelope of time-varying S curves in Figures 3(d) and 4(d) showed the steady patterns during the red light, with the disordered patterns during the green light.

While vehicles passed by in the adjacent lane (referenced at the 65-s mark in Figure 4(c)), there was a clear decrease in FS curves during the green-light signals. The lower-frequency range of the traffic light signals often gets masked by the more prominent low-frequency vehicle noise, which mirrors the rising trends of traffic noise observed in prior studies [18, 21]. This interference can lead to a shift in f_{mod}, resulting in a decrease in FS. Moreover, a modulation frequency of f_{mod} = 12.8 Hz was distinctive of traffic light signals. As indicated by the comparative data points, f_{mod} tended to be unstable at the intersections without traffic light signals, and FS values also diminished to a lower level as a result.

The difference in time-varying R observed in Figure 5 between the red-light and green-light signals primarily stemmed from the sound sources present (vehicle noise and traffic light signals), and f_{mod} was consistently around 12.8 Hz during the green-light signals. However, the majority of f_{mod} hovered within the 80–100 Hz range during the red-light signals, with only a few segments retaining the 12.8 Hz frequency. In contrast to FS values, vehicle noise can influence the perception of R, with f_{mod} typically rising within the low-frequency range (80–100 Hz). During the red-light signals, the increase of vehicle noise can overshadow the traffic light signals, and the variation in f_{mod} contributed to a slightly higher R during the red-light signals [22].

3.1.2 Analysis of rhythmic events

The concept of beats per minute (BPM) proves useful in quantifying the frequency of uniform fluctuations per minute in a stable signal [51, 52]. As shown in Figure 3(b and c), the pure traffic light signals (without random vehicle noise) presented the regular patterns in the loudness time-varying curves. Notably, the BPM of the pure green-light signals, set at 608 BPM, was eight times higher than that of pure red-light signals (BPM = 76) across all measurement points. Therefore, the concept of rhythmic events per minute (REPM) was defined to analyze the measured segments on a BPM scale. These rhythmic events were

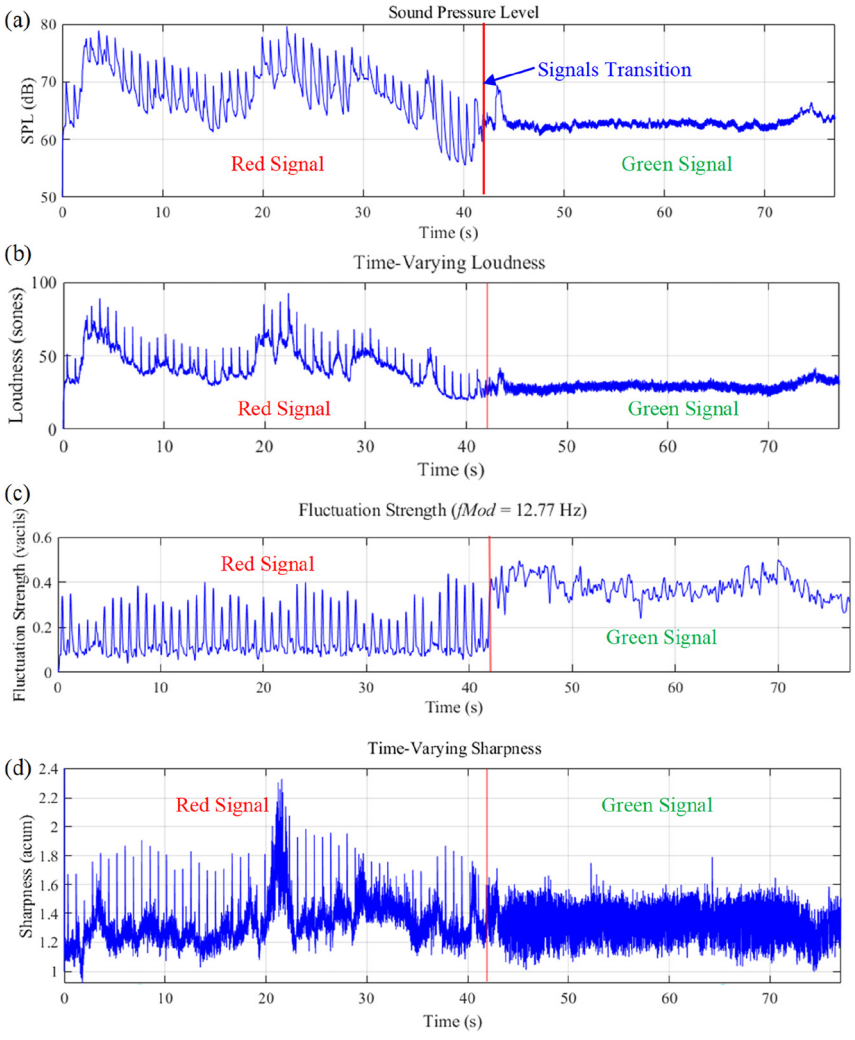

Figure 3: The time-varying curves of two consecutive measured segments (peak time measured at the point 2): (a) sound pressure level; (b) loudness; (c) fluctuation strength; (d) sharpness.

computed and categorized using the MATLAB function module. However, the REPM values for all green-light signals were disregarded due to the brief intervals. The intervals of green-light signals were less than the minimum perceptible time gap (120 ms) in Eq. (8).

The BPM value of 76 for red-light signals, as depicted in Figure 6, served as a notable threshold positioned within the upper interquartile range (IQR) of peak-time and overall segments, with the upper limit around BPM = 76 even during the off-peak hours. The dynamically changing time-varying loudness (N) and maximum loudness (N_{max}) derived from vehicle noise ultimately contribute to REPM values generally falling below BPM. Consequently, REPM was associated with stable red-light signals and lower sensitivity to vehicle noise. The presence of vehicle noise introduced instability, with a decrease of REPM. Nevertheless, the distinguishable rhythmic perceptions remained predominantly induced by the traffic light signals.

3.2 Spectral characteristics

The mel spectrogram in Figure 7 illustrated the specific loudness (N') at the critical band rate scale, emphasizing the spectral characteristics over time. The 10-s segments were selected to highlight the signal transition within a short duration. During the red-light signals, these frequencies appeared as a series of regular peaks, indicating consistent oscillations throughout the period, visualized as vertical-line patterns in Figure 7(b) and (d). In contrast, the green-light signals generated a more frequent vertical-line pattern, with a multiple of 8, aligning with the findings in Section 3.1.2. During the signal transition in Figure 7(c), both the red-light signals and the green-light signals produced distinct frequencies at 5, 13, 16, and 20 Bark. Moreover, a repeated measurement of the covered windscreen has verified that wind interference does not influence the distinct frequencies of traffic signals.

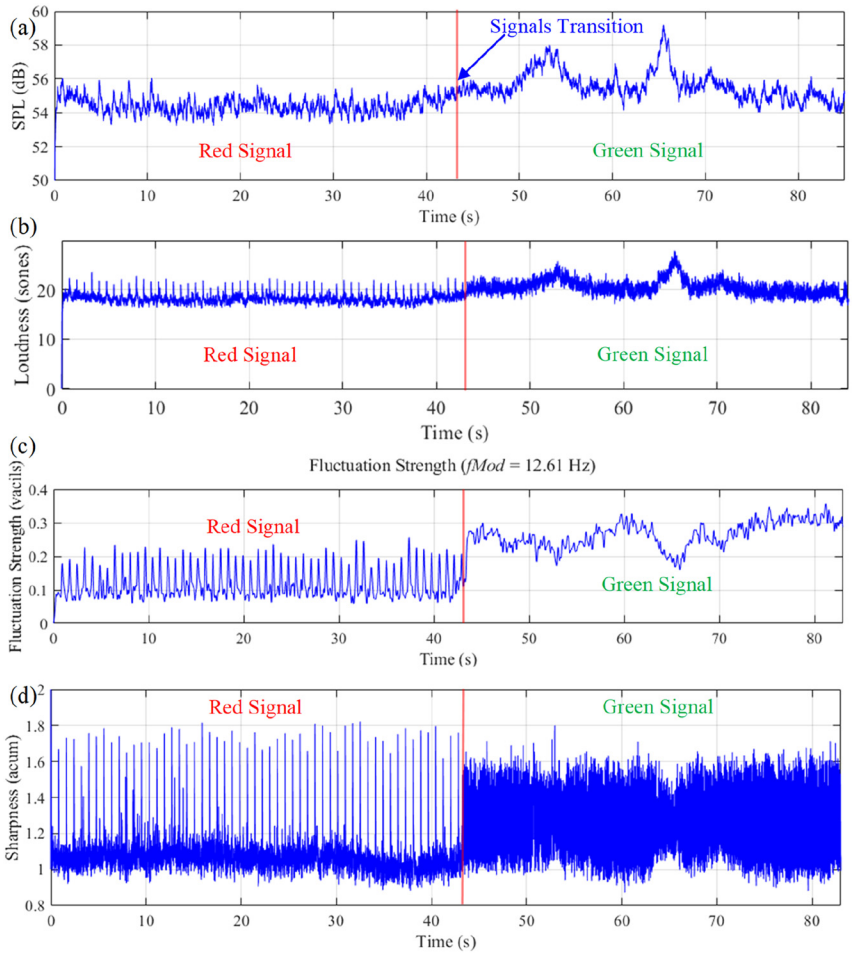

Figure 4: The time-varying curves of two consecutive measured segments (off-peak time measured at the point 2): (a) sound pressure level; (b) loudness; (c) fluctuation strength; (d) sharpness.

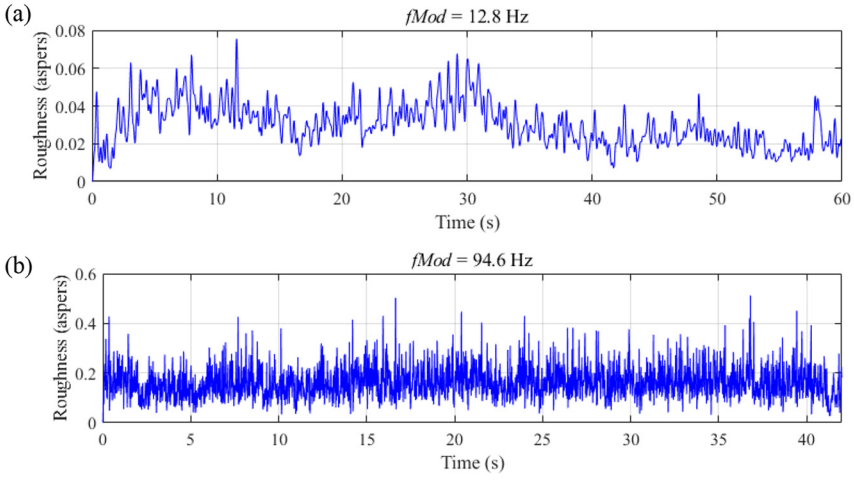

Figure 5: The time-varying curves of roughness (measured at the point 2): (a) green-light signal; (b) red-light signal.

Due to the lack of concurrent traffic data, Figure 7(a) and (e) selected the spectrograms for different traffic-light signals to visually illustrate the impact of vehicle noise. It indicated that the process of a vehicle passing through the intersection typically lasts no more than 5 s. During this time, N' values around 2 Bark increased significantly due to the vehicle, and a series of irregular peaks within the 0–10 Bark range can be observed in the spectrograms. Portions of the traffic signal's frequencies at 5 Bark were masked by random vehicle noise, but the high-frequency components at 16 and 20 Bark remained unaffected. Previous investigation of traffic noise consistently indicated that the high-frequency

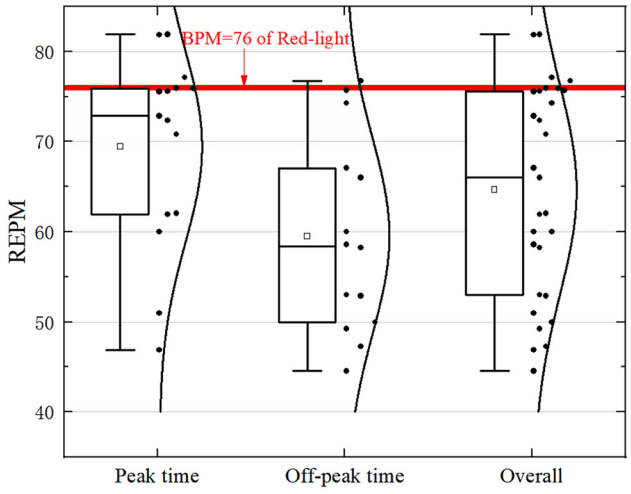

Figure 6: The calculated rhythmic event per minute (REPM) for all red-light segments.

proportion above 3,000 Hz of vehicle noise was extremely low [21].

In terms of the total duration, Figure 8 illustrated the mean N' values of different traffic light signals across critical-band rates for all segments. As shown in Figure 8(a and b), the N' values of peak time were significantly higher than that of off-peak time in the range of the entire 0–24 Bark. Meanwhile, N' around 2 Bark and 16 Bark showed an obvious elevation during the peak time compared to the off-peak time, but the elevations of N' around 5 Bark and 20 bark were not as pronounced as at two bark and 16 bark. The N' values around 2 Bark were slightly higher during the red-light signals due to the increased vehicle noise. However, the red-light and green-light signals were all concentrated around 16 Bark in spectral characteristics.

In Figure 9(a), the tone-to-noise ratio (TNR) highlighted a consistent prominent frequency of approximately 3,270 Hz within traffic noise, corresponding to N' at 16 Bark. The blue peak in Figure 9(a) also appeared at various characteristic frequencies at at 2,200 Hz (12 Bark), 6,500 Hz (20 Bark), and 10,000 Hz (23 Bark). The characteristic frequency range was consistent with the mel spectrogram results in Figure 7. Nevertheless, TNR values exhibited significant variation across different segments, with only a minority meeting the criteria for prominence tone as depicted in Figure 9(b). The reason is that the acoustic design of the traffic signal source also considered the repetition rate (temporal) characteristics [18, 19]. Moreover, the traffic light signals introduced a distinct tonal presence or spectral pattern, with high frequencies (around 16 Bark) being further influenced by vehicle noise in spectral perception [21]. Consequently, only a few segments characterized by low-level random vehicle noise surpassed the prominence tone threshold at 16 Bark.

4 Discussion

4.1 Statistical description for the measured indicators

According to the standard of traffic light signals (ISO 23600:2007), the sound pressure level of all traffic light signals should be maintained between +5 dB and +10 dB relative to the ambient noise level [53]. However, the perceptual differences were not explained between red-light and green-light signals due to the lack of psychoacoustic indicators. Table 4 presented the statistical outcomes for both psychoacoustic and traditional indicators across all segments in the measurement. The measurement revealed that the mean values of N_{eq}, N_5, N_{max}, L_{Aeq}, and L_{max} for both red-light and green-light signals were nearly identical. During the green-light signals, the mean and median values of most indicators were slightly higher than during the red-light signals.

The Shapiro-Wilk tests result indicated that two indicators (R and FS) do not follow a normal distribution ($p < 0.05$). The nonparametric tests (Mann-Whitney U test) were conducted to examine whether the indicators have significant differences between the green-light signals and the red-light signals. The null hypothesis was that there are no statistically significant differences in the subjective data for individual questions, and the effect size r was calculated by rank-biserial correlation [54]. Two indicators, S ($p = 0.011$, $r = 0.42$) and FS ($p < 0.001$, $r = 0.91$), showed significant differences for different traffic lights. However, the statistical distributions of S were still similar for different traffic lights in Figure 10(a) due to the same standard deviation and approximate mean. In contrast, the distributions of FS varied significantly for different traffic lights in Figure 10(b), with the distribution during the green-light signals being more dispersed than during the red-light signals.

4.2 Statistical description for subjective listening tests

A total of 24 segments from the aforementioned segments were further evaluated for the listening tests, with 12 segments from red-light signals and 12 segments from green-light signals. A questionnaire for one participant included six peak segments and two off-peak segments to consider the complex and

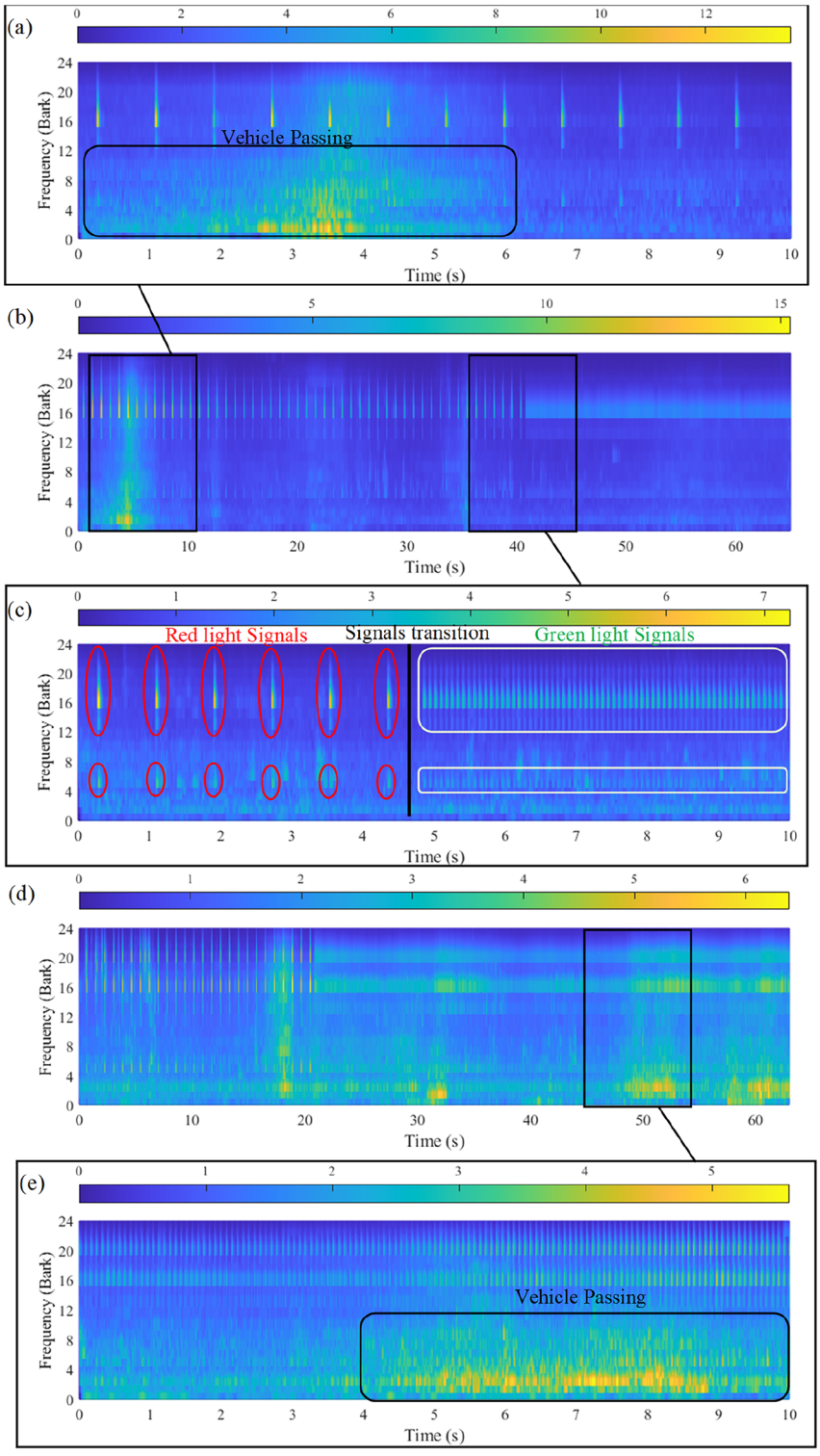

Figure 7: The mel spectrogram of the specific loudness (N'): (a–c) vehicle passing and signal transition at measured point 2; (d and e) vehicle passing at measured point 1.

random vehicle noise. 15 participants with 60 valid questionnaires were collected for the red and green light signals, respectively (sample size, n = 120). The reliability statistics of the questionnaires' results showed a good level of subjective results, with the Cronbach's Alpha coefficient at 0.885 [42].

Figure 11 presented the mean scores for various questions, categorized by the types of traffic lights. It can be seen that all results in the questionnaire had a positive value, so the acoustic environment at the intersections was annoying and unpleasant for participants. Question two exhibited a

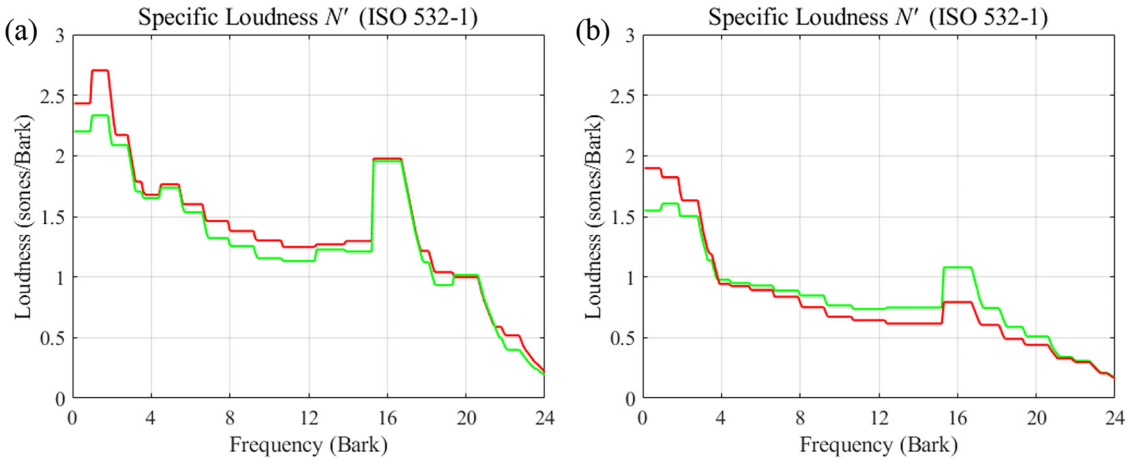

Figure 8: The mean specific loudness for all segments: (a) peak time; (b) off-peak. (The red and green lines denote the red and green-light signals respectively).

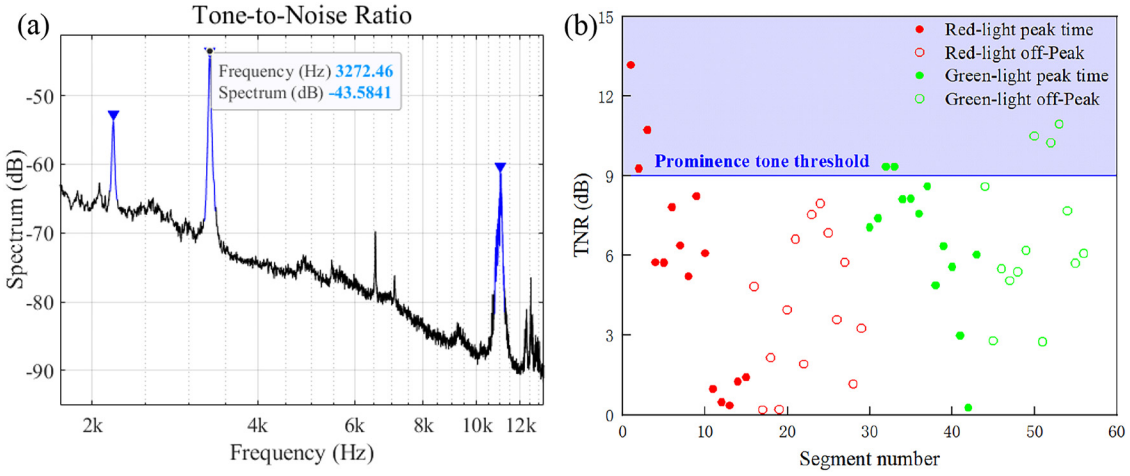

Figure 9: Tone-to-noise ratio results: (a) tone-to-noise ratio in frequency spectrum; (b) results of all segments with the prominence tone threshold.

Table 4: The statistical results of the measured indicators for all measured segments.

		N_{eq} sone	N_{max} sone	N_5 sone	PA	L_{Aeq} dB	L_{max} dB	S^a acum	FS^a vacil	R asper
Mean (±standard deviation)	Red	30.24	55.39	39.33	41.36	59.24	84.01	1.22	0.13	0.07
		(8.97)	(18.0)	(11.7)	(18.0)	(4.85)	(6.16)	(0.02)	(0.02)	(0.06)
	Green	30.43	55.09	39.22	42.04	59.35	83.86	1.31	0.29	0.05
		(9.40)	(20.0)	(12.4)	(12.9)	(5.32)	(6.76)	(0.09)	(0.09)	(0.01)
	Total	30.33	55.25	39.28	41.69	59.30	83.93	1.26	0.21	0.06
		(9.18)	(19.0)	(12.0)	(12.4)	(5.09)	(6.46)	(0.10)	(0.10)	(0.04)
Median	Red	34.18	59.29	42.42	43.69	61.29	84.75	1.24	0.13	0.06
	Green	32.05	57.89	41.32	46.18	60.08	84.48	1.30	0.27	0.05
	Total	32.05	58.85	42.42	43.69	60.08	84.65	1.28	0.17	0.05

[a]: Significant difference in Mann-whitney U test.

similar sensitivity to green-light signals (M = 1.60, SD = 1.21) compared to the red-light signals (M = 1.38, SD = 1.49), without the statistical significance (p = 0.375). Furthermore, Question 3 (sensitivity to vehicle noise) was slightly higher during the

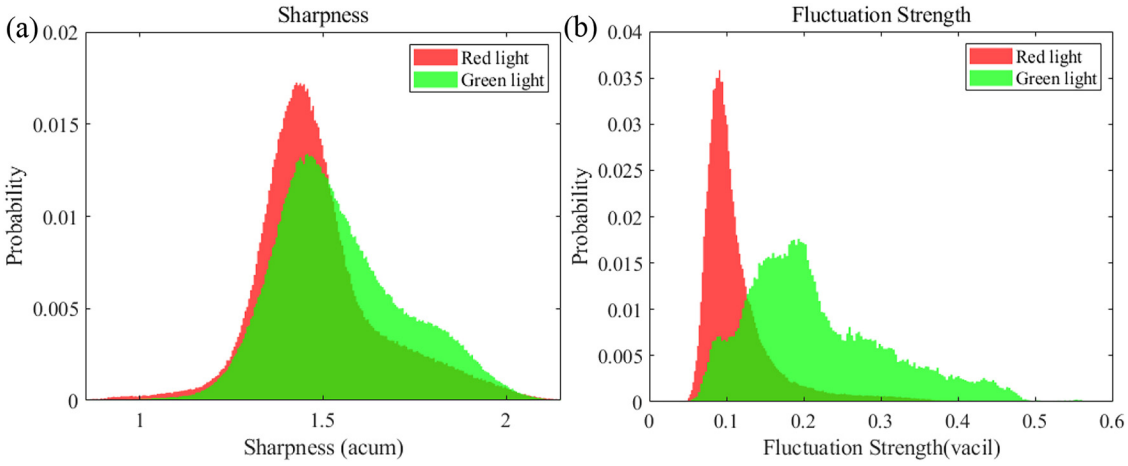

Figure 10: The probability distributions of significantly different indicators for all segments: (a) sharpness; (b) fluctuation strength.

red-light signals (M = 1.85, SD = 1.51) than the green-light (M = 1.70, SD = 1.61), but the result of Mann-Whitney U tests showed no significant difference between the two groups (p = 0.714). However, the score for most questions in the green-light signals was higher than that of the red-light signals, and Question 4 (sensitivity to traffic light) for the green-light signals (M = 1.83, SD = 1.52) was significantly greater than that of the red-light signals (M = 1.30, SD = 1.46, p = 0.038).

The Shapiro-Wilk tests indicated that all subjective data do not follow a normal distribution ($p < 0.05$). Consequently, the Mann-Whitney U tests were conducted to assess the statistical significance of the subjective data in Figure 11. The

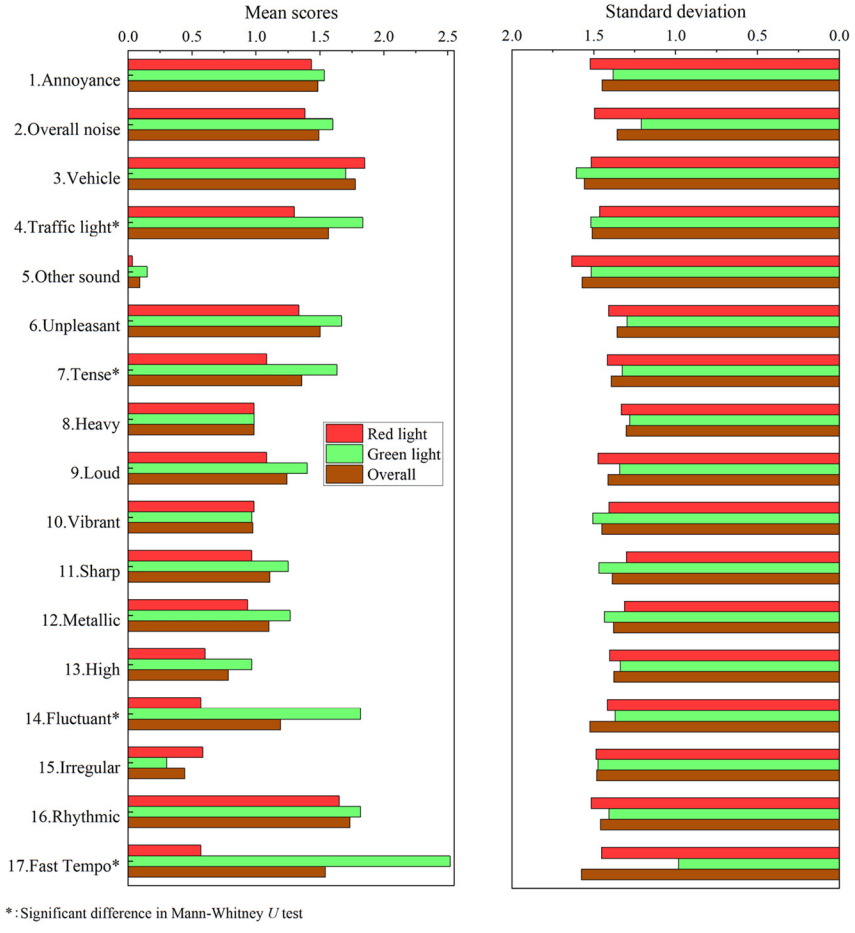

Figure 11: Mean scores and standard deviation of the subjective listening tests: questions 2–5 denote the sensitivities to different sounds, questions 6–17 denote the different perceptions.

perceptions of tense/relaxed (p = 0.032, r = 0.22), fluctuant/steady (p < 0.01, r = 0.48), and fast/slow tempo (p < 0.01, r = 0.71) rejected the null hypothesis, as well as the sensitivity to traffic light signals (p = 0.038, r = 0.22). Based on the aforementioned perceptions, participants in the listening tests can significantly distinguish traffic light signals during the signal transition. Prolonged exposure (over 30 s) to the green-light signals was associated with higher reported sensitivity and perception scores compared to the red-light signals.

4.3 Correlation analysis

A Spearman correlation analysis was conducted to explore the relationship between the subjective data and measured indicators. Figure 12 presented heatmaps showing the correlations between the measured indicators and the subjective data, and the heatmaps can be explained by three parts. Firstly, vehicle noise was highly correlated with the measured indicators N_{eq}, N_5, N_{max}, L_{Aeq}, L_{max}, R, PA (p < 0.01), and S (p < 0.05). The perceptions of tense/relaxed and loud/quiet showed the highest correlation with the intensity indicators N_{eq}, N_5, and L_{Aeq}. However, the correlations between vehicle noise and several other indicators (FS, TNR, and REPM) were relatively low, at −0.07, 0.17, and −0.18, respectively.

Secondly, the sensitivity to traffic light signals was correlated with all measured indicators except for R in Figure 12. The correlations of S, FS, TNR, and REPM with traffic light signals were significantly higher than with vehicle noise. The correlation coefficient between FS and the slow/fast tempo was the highest at 0.48. Therefore, a higher perception of a fast tempo was associated with higher FS values, which was in turn linked to higher sensitivity to traffic light signals. The increased perception of fast tempo was also consistent with the higher FS values during the green-light signals. Meanwhile, FS showed almost no correlation with vehicle noise and its corresponding perceptions (<0.10), and it was only correlated with the signal transition. The REPM had a correlation with sensitivity to traffic light (0.21) and significantly negative correlations with irregular/regular (−0.32), heavy/light (−0.28), and sharp/dull (−0.27).

Another study also identified elevated FS values in relation to construction noise generated by pile drivers and breaker machinery, with the time-varying loudness curves showing patterns similar to those of red-light signals [55]. However, several studies focused on the vehicle noise or train noise have not identified any sound sources directly associated with FS [30, 31]. Moreover, the subjective listening tests employed tempo-related descriptors, including non-stationary/stationary, continuous/intermittent, and non-periodic/periodic, which were significantly associated with FS values [55]. The findings suggested that variations in FS

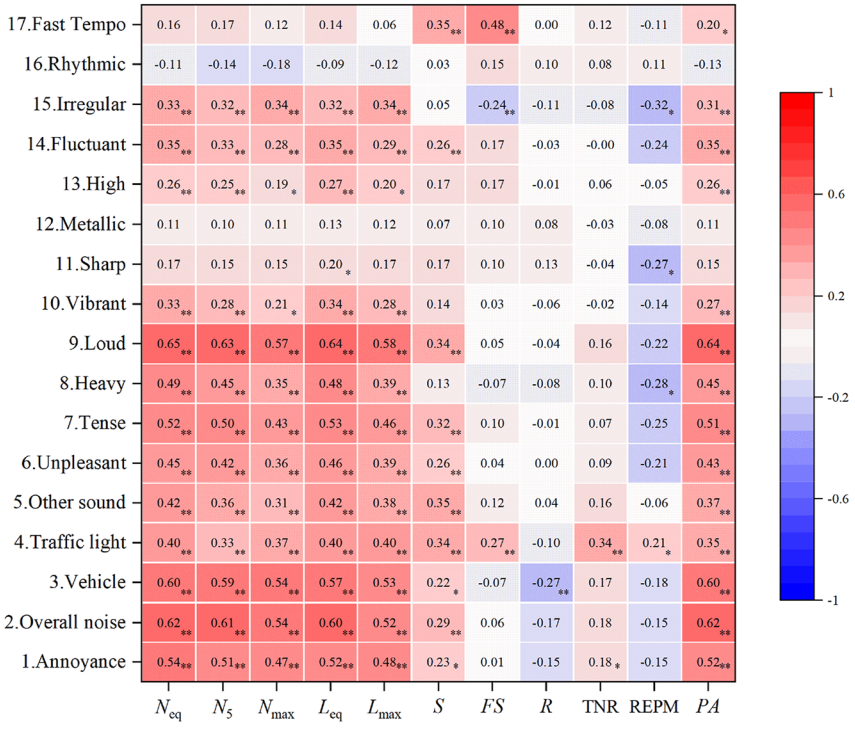

**: correlation is significant at the 0.01 level (2-tailed).

*: correlation is significant at the 0.05 level (2-tailed).

Figure 12: The heatmaps of the correlations between the measured indicators and the questions of the listening tests (REPM indicator only considered red-light signals).

may serve as a reliable independent indicator for evaluating the signal transition of traffic lights. The standard ISO 23600-2007 did not provide a specific description of the signal transition [53]. In summary, the temporal indicators (FS and REPM) effectively captured temporal variance over time, which was significantly correlated with perceived rapid tempo and regularity.

Finally, *S* also shows a high correlation with two temporal-related perceptions, likely due to the strong correlation (0.55) between the measured indicators FS and *S*. Additionally, while the correlation between TNR and sensitivity to traffic noise was high (0.34), its correlation with multiple perceptions in the questionnaire was relatively weak. Another study also identified the frequency of traffic noise and signal sounds, which all widely ranged from 400 to 3,000 Hz [21]. The overlapped spectral characteristics of traffic signal sounds are highly susceptible to interference from random traffic noise. Changing spectral indicators (*S*, *R*, and TNR) can significantly affect sensitivity, but temporal indicators provided clearer perception for distinguishing between the red-light and green-light signals [20].

5 Limitation and future work

The single type of traffic-light signal was the limitation in this study due to the geographic restriction (only in Hong Kong), and the measured points were also limited to four intersections. To increase the generality of the findings, field measurements and subjective surveys in different cities or regions are necessary to analyze various traffic-light signals (e.g., bird sounds or water sounds) in future work. Therefore, future studies will consider the influence of signal-typed sounds in different acoustic environments.

This study conducted a pre-measurement, and a repeated measurement was also conducted with the microphone covered by the windscreen. The results showed the negligible differences of conclusion under the condition without a windscreen in low wind speed. However, the formal measurement (without the windscreen) may introduce low-frequency acoustic interferences, affecting some acoustic indicators. Therefore, the windscreen protection is necessary for future measurements.

The selected intersections are exploratory in this study due to the complex traffic information and road geometry in Hong Kong. The complex geometry conditions, including various surrounding buildings (maybe low-rise buildings), road types (pavement materials or lane width), and different traffic flow, will potentially influence the acoustic perceptions of traffic-light signals. Moreover, relying solely on AADT and speed limits does not capture the dynamic traffic data of volume, composition (heavy/light vehicles), and speed during the acoustic measurements. These variables will potentially affect temporal (REPM) and spectral (TNR, Bark) patterns. Therefore, on-site traffic counts were identified as a critical area for improvement in future research, where the synchronized video cameras and environmental survey will be conducted in future studies.

Only 15 listeners were included in the listening tests, and the participants' age and familiarity with the emotional state were not considered in the tests. The temperature variation and visual elements in the outdoor environment were not considered in the indoor listening test. Moreover, the correlations between different subjective descriptors have not been discussed due to the limited content. The potential influence of different scenarios on the participants' sensory experiences deserves discussion in future work.

According to Eqs. 9–11, psychoacoustic annoyance (PA) is predominantly calculated by the loudness indicator N_5. Therefore, the effectiveness of PA was influenced by random vehicle noise when evaluating the differences between the red-light and green-light signals. The suitability of the PA indicator for assessing transient, signal-based sounds rather than steady-state noise should be analyzed in future studies.

6 Conclusions

The pattern changes of traffic light signals were qualitatively identified in the various psychoacoustic time-varying curves (*N*, *S*, FS, and *R*). After that, the significant changes of the mean FS value during the signal transition quantitatively demonstrated the changes in the temporal characteristics. The spectral characteristics (*N*′ and TNR) showed that the traffic-light signals produce specific frequencies at 5, 13, 16, and 20 Bark. A repeated measurement of the covered windscreen has verified that wind interference does not influence the distinct frequencies of traffic signals. Moreover, the corresponding frequency range of the random vehicle noise is concentrated below 10 Bark, and the high-frequency components of traffic-light signals over 16 Bark remain unaffected by random vehicle noise. The subjective listening tests further showed that the sound sensitivity to the red-light and green-light signals was significantly different. The temporal perceptions were significantly correlated with temporal indicators FS and REPM. In

contrast, the sensitivity to vehicle noise was only found to be significantly correlated with the intensity indicators (*N* and SPL) and spectral indicators (*S* and *R*), but not the temporal indicators.

The discussion revealed temporal indicators (FS and REPM) are paramount for characterizing the perception of signal transitions. However, previous investigations of traffic noise focused on intensity indicators (*N* and SPL) are insufficient to explain the acoustic perceptions at the intersections. The ISO standard of traffic light signals does not incorporate the psychoacoustic indicators, leaving a potential direction for policy development. Based on the deficiency of the SPL indicator, the psychoacoustic indicators (e.g., FS and REPM) should be initially adopted as complementary design guidelines for optimizing signal perception. In the future, the formal standards can be integrated with the psychoacoustic indicators in outdoor environments. The local administration should preliminarily evaluate the feasibility and implementation challenges due to the necessity of advanced equipment and technology. Thus, this study conducted both the exploratory measurement and data analysis to advance the evaluation and design of acoustic signals in noisy environments.

Funding information: The work described in this paper was fully supported by a grant from the Research Grants Council of the Hong Kong Special Administrative Region, China (PolyU15212822).

Author contributions: All authors have accepted responsibility for the entire content of this manuscript and consented to its submission to the journal, reviewed all the results and approved the final version of the manuscript. DSP contributed in writing, analysis of data, test design and test development; CMM contributed in funding and conceptualization; MKW contributed in analysis of data, test development, and conceptualization; GL contributed in test development.

Conflict of interest: Authors state no conflict of interest.

Data Availability Statement: The datasets generated during and/or analysed during the current study are available from the corresponding author on reasonable request.

Appendix A: Detailed parameters of calculations and measurement information

Tables 5 and 6

Table 5: Detailed indicators of calculations and acquisition settings in MATLAB 2024b.

	Detailed parameters	Values (units)	Note
Acquisition settings	Sample rate	48 kHz	
	Bit depth	24-bit	
	Audio format	WAV (uncompressed)	
Mel spectrogram settings	Window type	Hann	
	Overlap length	512 (default)	
	FFT length	1,024 (default)	
Acoustic implementation	SLM-frequency weighting	A-weighting	Applied for L_{eq}
	SLM-time weighting	Fast	Applied for L_{max}
Psychoacoustic implementation	Number of critical bands	47 (1/2 bark)	Applied for *N*, *S*, *R*, FS
	Modulation frequency (f_{mod})	Auto-detect (default)	Applied for *R* and FS
	Time-varying output resolution (*N*(t))	2 ms (500 Hz)	Applied for *N*, *S*, *R*, FS

Table 6: The traffic information of selected road intersections.

Measured point	Number of lane size	Building façade distances	Measured points' location	Traffic-light number
1	3/4/4/4	2.3 m	Roadside	10
2	2/3/4/4	5.0 m	Roadside	6
3	2/4/5/6	16.1 m	Refuge island	16
4	2/3/5/6	13.7 m	Refuge island	8
5	2/2/4	4.8 m	Roadside	–

1. Number of lane size: The number of lanes on each of the four (three) roads connected to intersection, with each lane having a standard width of 3.5 m. 2. Building façade distances: The minimum distance from surrounding buildings to the roadside or refuge island. 3. Traffic-light number: the total number of traffic lights that generate signal sounds.

References

1. Brown AL, Lam KC. Levels of ambient noise in Hong Kong. Appl Acoust 1987;20:85–100.
2. Yang X, Han Z, Lu X, Zhang Y. A rapid approach to urban traffic noise mapping with a generative adversarial network. Appl Acoust 2025;228: 110268.
3. European Environment Agency. Environmental noise in Europe – 2020. Luxembourg: Publications Oflce of the European Union; 2014.
4. World Health Organization. WHO environmental noise guidelines for the European Region. Copenhagen: WHO Regional Office for Europe; 2019.
5. Morillas JMB, Gozalo GR, González DM, Moraga PA, Vílchez-Gómez R. Noise pollution and urban planning. Curr Pollut Rep 2018;4:208–19.

6. Patel R, Singh PK, Saw S, Tiwari S. Assessment and prediction of noise pollution–induced health impacts in urban environment: a structural equation modeling (SEM)–based approach. Arabian J Geosci 2024;17: 305.
7. Tiwari SK, Kumaraswamidhas LA, Garg N. Assessment of noise pollution and associated subjective health complaints in Jharia Coalfield, India: a structural equation model analysis. Noise Mapp 2023;10:2022–0172.
8. Lam KC, Chan PK, Chan TC, Au WH, Hui WC. Annoyance response to mixed transportation noise in Hong Kong. Appl Acoust 2009;70: 1–10.
9. Cai C, Mak CM, He X. Analysis of urban road traffic noise exposure of residential buildings in Hong Kong over the past decade. Noise Health 2019;21:142–54.
10. Law C, Lee C, Lui AS, Yeung MK, Lam K. Advancement of three-dimensional noise mapping in Hong Kong. Appl Acoust 2011;72: 534–43.
11. Abo-Qudais S, Alhiary A. Statistical models for traffic noise at signalized intersections. Build Environ 2007;42:2939–48.
12. Song J, Meng Q, Kang J, Yang D, Li M. Effects of planning variables on urban traffic noise at different scales. Sustain Cities Soc 2024;100: 105006.
13. Li F, Lin Y, Cai M, Du C. Dynamic simulation and characteristics analysis of traffic noise at roundabout and signalized intersections. Appl Acoust 2017;121:14–24.
14. Patel R, Singh PK, Saw S. Traffic noise modeling under mixed traffic condition in mid-sized Indian City: a linear regression and neural network-based approach. Int J Math Eng Manag 2024;9: 411–34.
15. Patel R, Singh PK, Saw S. A modeling approach for suitability evaluation of traffic noise prediction under mixed traffic situation in mid-sized Indian cities. Innovat Infrastruct Solut 2024;9:183.
16. Szeto AY, Valerio NC, Novak RE. Audible pedestrian traffic signals: part 2. Analysis of sounds emitted. J Rehabil Res Dev 1991;28:65–70.
17. Notbohm G, Västfjäll D, Gärtner C, Schwarze S. Subjective evaluation of the sound quality of urban traffic noise situations. In: Proceedings of the 18th ICA; 2004.
18. Bogusz E, Furmann A. Psychoacoustical estimation of selected acoustic signals which can be applied at pedestrian crosswalks. Acta Phy Pol A 2011;119:925–31.
19. Niewiarowicz M, Furmann A. Localization of acoustic signals used in sound emitters at pedestrian crosswalks. Acta Phy Pol A 2012;121: 9–12.
20. Koh PP, Wong YD, Menon APG. Acceptability of audible pedestrian signal noise. Transport Res D-Tr E 2012;17:179–83.
21. Trollé A, Terroir J, Lavandier C, Marquis-Favre C, Lavandier M. Impact of urban road traffic on sound unpleasantness: a comparison of traffic scenarios at crossroads. Appl Acoust 2015;94:46–52.
22. Can A, Leclercq L, Lelong J. Acoustic descriptions for dynamic noise estimation close to traffic signals. In: Inter-noise congress and conference proceedings; 2007.
23. Zwicker E, Fastl H. Psychoacoustics: facts and models. Germany: Springer Science & Business Media; 2013.
24. Aletta F, Oberman T, Mitchell A, Tong H, Kang J. Assessing the changing urban sound environment during the COVID-19 lockdown period using short-term acoustic measurements. Noise Mapp 2020;7: 123–34.
25. Ma KW, Mak CM, Wong HM. Effects of environmental sound quality on soundscape preference in a public urban space. Appl Acoust 2021;171: 107570.
26. Brambilla G, Gallo V, Asdrubali F, D'Alessandro F. The perceived quality of soundscape in three urban parks in Rome. J Acoust Soc Am 2013;134: 832–9.
27. Ma KW, Wong HM, Mak CM. A systematic review of human perceptual dimensions of sound: meta-analysis of semantic differential method applications to indoor and outdoor sounds. Build Environ 2018;133: 123–50.
28. Ma KW, Mak CM, Wong HM. Acoustical measurements and prediction of psychoacoustic metrics with spatial variation. Appl Acoust 2020;168: 107450.
29. Mak CM, Ma KW, Wong HM. Prediction and control of noise and vibration from ventilation systems. 9781032061986. Boca Raton: CRC Press; 2023.
30. Gille LA, Marquis-Favre C. Estimation of field psychoacoustic indices and predictive annoyance models for road traffic noise combined with aircraft noise. J Acoust Soc Am 2019;145:2294–304.
31. Nowakowski T, Komorski P. Tram noise annoyance: the role of different psychoacoustic measures in the assessment of noise. Appl Acoust 2024;219:109946.
32. Can A, Leclercq L, Lelong J, Defrance J. Capturing urban traffic noise dynamics through relevant descriptors. Appl Acoust 2008;69:1270–80.
33. Caclina A, Giard M, Smith BK, McAdams S. Interactive processing of timbre dimensions: a garner interference study. Brain Res 2007;1138: 159–70.
34. Räsänen O, Laine UK. Time-frequency integration characteristics of hearing are optimized for perception of speech-like acoustic patterns. J Acoust Soc Am 2013;134:407–19.
35. Saitis C, Siedenburg K. Brightness perception for musical instrument sounds: relation to timbre dissimilarity and source-cause categories. J Acoust Soc Am 2020;148:2256–66.
36. Siedenburg K, Saitis C, McAdams S, Popper AN. Timbre: acoustics, perception, and cognition. Cham, Switzerland: Springer International Publishing; 2019.
37. Grondin S. Timing and time perception: a review of recent behavioral and neuroscience findings and theoretical directions. Atten Percept Psycho 2010;72:561–82.
38. Grassi M, Mioni G. Why are damped sounds perceived as shorter than ramped sounds. Atten Percept Psycho 2020;82:2775–84.
39. Köhlmann M. Rhythmische Segmentierung von Sprach-und Musiksignalen und ihre Nachbildung mit einem Funktionsschema. Acta Acust United Ac 1984;56:193–204.
40. Liang P, Guan H, Wang Y, Chen H, Song P, Ma H, et al. The effect of music tempo and volume on acoustic perceptions under the noise environment. Sustainability 2021;13:4055.
41. International Organization for Standardization. ISO 532-1: 2017 acoustics – Methods for calcualting loudness - part 1: Zwicker method, Geneva; 2017.
42. Deutsches Institut für Normung. DIN 45692 Measurement technique for the simulation of the auditory sensation of sharpness. Berlin: DIN; 2009.
43. Møller C, Stupacher J, Celma-Miralles A, Vuust P. Beat perception in polyrhythms: time is structured in binary units. PLoS One 2021;16: e0252174.
44. ECMA-418-1. Psychoacoustic metrics for ITT equipment – part 1 (prominent discrete tones). Ecma International.
45. Ma KW, Mak CM, Wong HM. Development of a subjective scale for sound quality assessments in building acoustics. J Build Eng 2020;29: 101177.
46. International Organization for Standardization. ISO/TS 12913-3: 2019 acoustics – Soundscape – Part 3: data analysis, Geneva; 2019.

47. Alsina-Pagès RM, Parés ME, Vidaña-Vila E, Freixes M, Garcia D, Arnela M, et al. Conscious walk assessment for the joint evaluation of the soundscape, air quality, biodiversity, and comfort in Barcelona. Noise Mapp 2024;11:20220182.
48. Li M, Han R, Xie H, Zhang R, Guo H, Zhang Y, et al. Mandarin Chinese translation of the ISO-12913 soundscape attributes to investigate the mechanism of soundscape perception in urban open spaces. Appl Acoust 2024;215:109728.
49. Jeon JY, Lee J, Hong J, Cabrera D. Non-auditory factors affecting urban soundscape evaluation. J Acoust Soc Am 2011;130:3761–70.
50. Sudarsono AS, Lam YW, Davies WJ. The effect of sound level on perception of reproduced soundscapes. Appl Acoust 2016;110: 53–60.
51. Heslegrave RJ, Ogilvie JC, Furedy JJ. Measuring baseline-treatment differences in heart rate variability: variance versus successive difference mean square and beats per minute versus interbeat intervals. Psychophysiology 1979;16:151–7.
52. Scheirer ED. Tempo and beat analysis of acoustic musical signals. J Acoust Soc Am 1998;103:588–601.
53. International Organization for Standardization. BS ISO 23600:2007 assistive products for persons with vision impairments and persons with vision and hearing impairments – acoustic and tactile signals for pedestrian traffic lights, Geneva; 2007.
54. Kerby DS. The simple difference formula: an approach to teaching nonparametric correlation. Compr Psychol 2014;3. https://doi.org/10.2466/11.it.3.1.
55. Hong JY, Lam B, Ong ZT, Ooi K, Gan WS, Lee S. A multidimensional assessment of construction machinery noises based on perceptual attributes and psychoacoustic parameters. Autom ConStruct 2022;140: 104295.